GEOLOGY | THE GEOLOGICAL SOCIETY OF AMERICA®

https://doi.org/10.1130/G50277.1

Manuscript received 1 April 2022
Revised manuscript received 8 August 2022
Manuscript accepted 12 August 2022

Published online 4 November 2022

Rapid megaflood-triggered base-level rise on Mars

Joshua Ahmed[1]*, Jeffrey Peakall[2], Matthew R. Balme[3] and Daniel R. Parsons[1]
[1]Energy and Environment Institute, University of Hull, Hull HU6 7RX, UK
[2]School of Earth and Environment, University of Leeds, Leeds LS2 9JT, UK
[3]Department of Physical Sciences, Open University, Walton Hall, Milton Keynes MK7 6AA, UK

ABSTRACT

The existence of ancient fluvial systems on Mars is widely accepted, but little is known about how quickly they formed, or what environmental conditions controlled their evolution. We analyzed a sequence of well-preserved inner-bank bar deposits within the meander bends of a multistacked sinuous fluvial ridge in Aeolis Dorsa and compared them to similar features on Earth to establish the conditions required for their formation. Our results reveal that these Martian channels were highly aggradational, rising an order of magnitude higher than terrestrial rivers. This evolution occurred over very rapid time scales, with our estimates suggesting that some entire inner-bar set deposits, and therefore the aggradational channel, may have formed in less than a single Martian year, with upper bounds of a few decades. We suggest that this unique channel topography was created by a rapidly rising downstream water body, triggered by a sequence of externally sourced megafloods (e.g., crater lake breaches).

INTRODUCTION

Evidence for megafloods is preserved in the Martian stratigraphic record and they are believed to have formed by the release of vast amounts of water from breached surface-water lakes or from rapid groundwater pressurization (Irwin et al., 2004; Rodriguez et al., 2015). Although these preserved erosional landforms offer some insight into the magnitude of the formative floods, they provide limited insights into the temporal evolution of the megafloods and their associated impact on local and global base-level rise (Larsen and Lamb, 2016). Contrastingly, on long-lived terrestrial fluvial systems, base-level changes are known to alter the channel's flow hydrodynamics, which in turn produces distinct sedimentary sequences that are archived in the stratigraphic record (Blum and Aslan, 2006). We propose that inner-bank bar deposits from a series of well-preserved meander bends in Aeolis Dorsa, Mars, formed during a series of megafloods, capturing and preserving the temporal dynamics of the system.

Meandering rivers are characterized by frequently changing geometries and distinct sedimentary accumulations at the insides of their bends, termed point bars (e.g., Constantine et al., 2014). Point bars grow during discrete flood events as sediment eroded from the outer banks is transported and deposited over the bar surface and on its margins (Peakall et al., 2007; Mason and Mohrig, 2019). This produces lateral accretion surfaces (LASs) that combine to form lateral accretion packages (LAPs); these have an undulating upper surface in exhumed point bars (Hayden and Lamb, 2020). Because the formation and scaling of these deposits are indicative of the prevailing environmental conditions, they can be used to infer past hydrological behavior and to identify signatures of environmental change (Blum and Aslan, 2006).

On Mars, the presence of well-preserved fluvial deposits across Aeolis Dorsa makes it ideal for exploring mechanisms of channel formation. Cardenas et al. (2018) interpreted 10 inverted sinuous ridges as exhumed incised-valley fills associated with ~50 m base-level oscillations driven by a dynamic downstream basin. This premise was supported by Hughes et al. (2019), who presented detailed measurements from an extensive delta system situated downstream of the inverted ridge deposits. However, despite the recognition of an ancient basin in Aeolis Dorsa, the trigger, extent, and evolutionary time scale remain unresolved. We present topographic measurements from a series of meander LAPs on a stacked channel in Aeolis Dorsa (AD1; Fig. 1) using a High Resolution Imaging Science Experiment (HiRISE) (McEwen et al., 2007) digital elevation model (DEM), and compare them to terrestrial deposits to postulate their formative conditions and time scales of formation.

METHODS

AD1 is composed of meanders with well-defined inner-bank growth increments, interpreted here as LASs (Mason and Mohrig, 2019), which show a consistent orientation with respect to the cap rock of the sinuous ridge (Fig. 1). This morphology in combination with the completeness of the LASs, which are indicative of bend expansion, indicate that these deposits represent channels rather than channel belts (cf. Hayden et al., 2019). At least two channels are stacked vertically over a streamwise distance of 22.6 km (Fig. 1; Fig. S1 in the Supplemental Material[1]). We inferred the position of the most recent active channels by digitizing the cap rock from a 1-m-resolution HiRISE DEM and used this to estimate channel width. The 17 best-preserved meanders were used for cross-sectional topographic analysis. Topographic profiles emanated from the inner part of the bend, extended across the LAPs and onto the channel crest, and terminated at the highest elevation relative to the starting point (Fig. 2A; Fig. S2). Relative elevation differences were measured from each profile and averaged at 1 m intervals (Fig. 2B). Cross-LAP slopes were calculated by dividing the maximum relative elevation change along the profile by the distance (Fig. 2C).

LASs were identified as topographic peaks along cross-LAP transects on well-preserved regions of each LAP (Fig. S3; Table S1). LAS elevations were extracted from equidistant

*E-mail: geomorphicjosh@gmail.com

[1]Supplemental Material. Detailed methodological approaches and rationale for calculations and deposit interpretations for channel AD1 (Aeolis Dorsa, Mars). Please visit https://doi.org/10.1130/GEOL.S.21191146 to access the supplemental material, and contact editing@geosociety.org with any questions.

CITATION: Ahmed, J., Peakall, J., Balme, M.R., and Parsons, D.R., 2023, Rapid megaflood-triggered base-level rise on Mars: Geology, v. XX, p. , https://doi.org/10.1130/ G50277.1

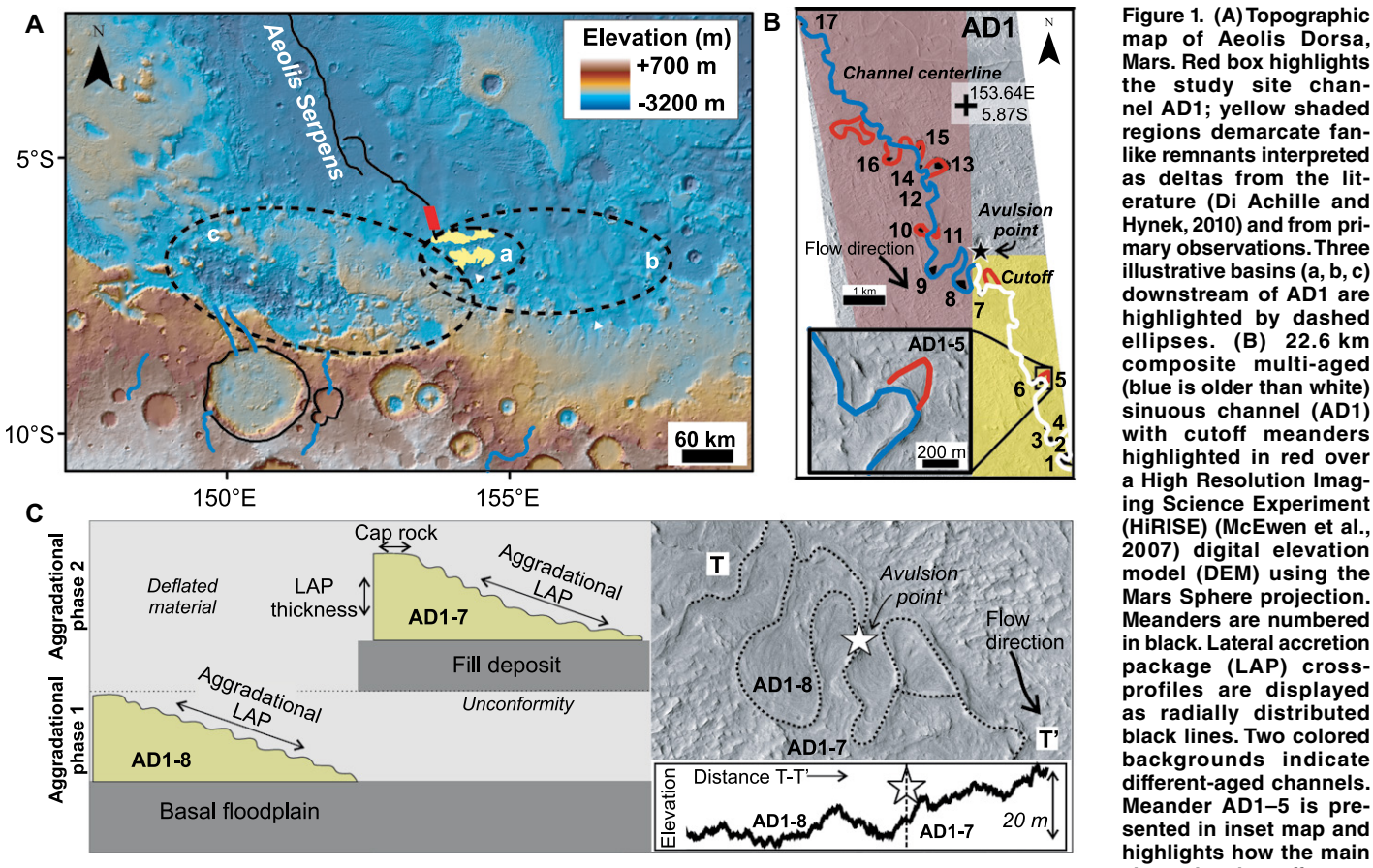

Figure 1. (A) Topographic map of Aeolis Dorsa, Mars. Red box highlights the study site channel AD1; yellow shaded regions demarcate fan-like remnants interpreted as deltas from the literature (Di Achille and Hynek, 2010) and from primary observations. Three illustrative basins (a, b, c) downstream of AD1 are highlighted by dashed ellipses. (B) 22.6 km composite multi-aged (blue is older than white) sinuous channel (AD1) with cutoff meanders highlighted in red over a High Resolution Imaging Science Experiment (HiRISE) (McEwen et al., 2007) digital elevation model (DEM) using the Mars Sphere projection. Meanders are numbered in black. Lateral accretion package (LAP) cross-profiles are displayed as radially distributed black lines. Two colored backgrounds indicate different-aged channels. Meander AD1–5 is presented in inset map and highlights how the main channel and cutoff meanders were identified. (C) Schematic of a multi-age channel with streamwise topographic profile between AD1–8 and AD1–7 (T–T′).

points (Fig. S4), and the 90th percentile was used as a representative value, since surface erosion disproportionately skews elevations to lower values. Intra-LAS elevation changes were computed as the difference between successive LAS elevations (Fig. 3A).

Estimates of AD1 channel depth, H (~1.8 m), and other hydraulic geometry parameters were made from empirical relationships (e.g., Konsoer et al., 2018; see the Supplemental Material and Fig. S5). Illustrative basins were identified at the downstream end of AD1 from the Mars Orbiter Laser Altimeter (MOLA) DEM (USGS, 2020) from outcrops of preserved ancient terrain (Fig. 1A). The extent of each basin was estimated and combined with the aggradational deposit depths from AD1 to calculate required volumes necessary to raise the basin level by an equivalent amount.

CHANNEL EVOLUTION AND FORMATIVE CONDITIONS

Relative LAP elevation changes varied from 0.3 to 14.4 m, with an average of 5.7 m (Fig. 2B); the absolute vertical resolution was ±0.5 m, although the spatial correlation of the data means that relative error will be far less (Palm et al., 2021). These changes equated to LAP slopes of 0.002 to 0.13 ± 0.006 based on absolute vertical resolution (Fig. 2C). Median between-LAS elevation changes varied between −0.3 and 1.2 m, with individual increases of >3 m (Fig. 3A). These elevation gains may be conservative in the absence of compaction and erosion estimates. The observed LAP elevation changes are far in excess of known increases in terrestrial systems (e.g., Durkin et al., 2015, their figure 11A). Critically, LAP thicknesses are multiples of the estimated channel depth, indicating that the observed inner bend morphology and topography are not the product of differential erosion of a single extremely thick LAP from a deep channel, but rather they are the product of exceptional channel aggradation. This aggradation can be quantified using a superelevation index (S_E) that measures the change in height between the lowest point of the inner-bend deposits and the cap-rock crest, h_i, accounting for the LAP thickness at the basal point ~H (Leeder, 1973), to give $h_i + H$, normalized by channel depth H (Fig. S5). S_E values ranged between 1.8 and 8.0 for AD1.

The closest terrestrial analogues displaying aggradation of this magnitude are submarine channels, where the relatively small density difference between the formative gravity current and ambient seawater reduces the propensity for channel avulsion (Peakall et al., 2000). However, comparing S_E for AD1 with both subaerial and submarine terrestrial channels (Jobe et al., 2020), we found that median S_E values for AD1 are 2.1 × larger than values for submarine channels and 37 × larger than values for subaerial channels (Fig. 3B; Tables S2 and S3). Superelevation potential is enhanced in submarine environments, where the effective gravity is approximately three orders of magnitude lower than at the surface, and, while gravity on Mars is ~38% of that on Earth, it is unlikely to be responsible for creating the extreme channel topography of AD1.

Stratigraphic evidence from the wider Aeolis Dorsa region revealed multiple delta lobes downstream of AD1, suggesting that it may have been a feeder channel to a delta system (e.g., Cardenas et al., 2018; Hughes et al., 2019) supplied with water from episodic rainfall events (Kite et al., 2019). We suggest that the formation of AD1's exceptional vertical relief was likely triggered by water-level rise in a downstream reservoir that forced the channel bed to aggrade to maintain equilibrium. Because there are at least two stacked channels characterized by rapidly rising LAS deposits (Fig. 1C), this aggradation must have occurred more than once.

We estimated the active life span of AD1, using an empirically derived Martian meander

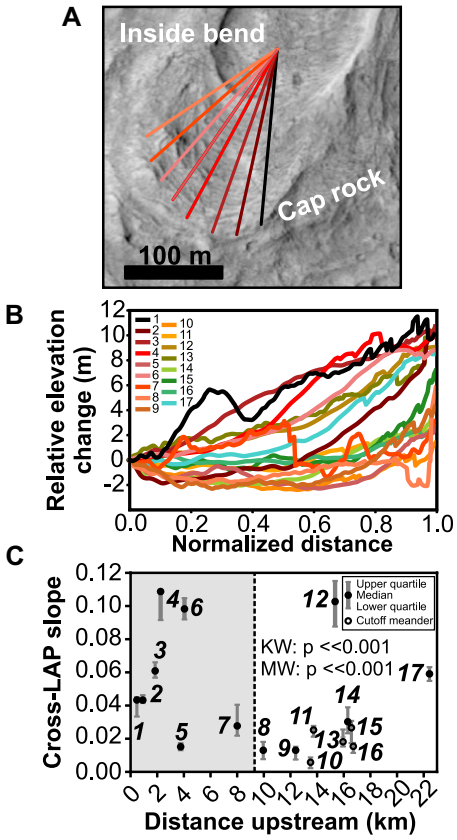

Figure 2. Lateral accretion package (LAP) cross-profile characteristics of channel AD1 (Aeolis Dorsa, Mars). (A) Individual topographic profiles for meander AD1–7. (B) Average cross-sectional topographic profiles for LAP deposits on AD1 bends 1–17. Abrupt changes in elevation on each averaged plot are artifacts of profile averaging caused by the decrease in number of profiles being averaged at that distance; these errors do not propagate. (C) Median LAP slopes bound (error bars) by lower and upper quartile slopes from population of transects. Shaded gray zone has statistically steeper slopes than the unshaded region. Kruskal-Wallis (KW) and Mann-Whitney *U*-test (MW) confidence values (*p*) are displayed for comparison of slopes in each zone. Filled points are main-stem meanders; open points are cutoff meanders.

migration model (Lapôtre and Ielpi, 2020) developed from a global compilation of barren channel migration rates, and 38 measurements of AD1 cap-rock channel width (see the Supplemental Material). Substituting channel width (B) for the estimated 10th, 50th, and 90th percentile widths, we estimated instantaneous bankfull migration rates (under the assumption of continuous bankfull flows) to be between 132 and 326 m yr^{-1} (Earth years) for AD1, which is similar to the range of distances over which the LAP profiles were measured (93–369 m), suggesting that each aggradational phase may have been accomplished, at a minimum, within a single Earth year before avulsing to a new location (see the Supplemental Material; Fig. S6; Tables S4 and S5). Flow intermittency, I, estimates for Mars, measured over 10^5–10^6 Martian years (Mars-yr) suggest bankfull frequency of 1 Martian day (sol) per ~2–18 Mars-yr (Buhler et al., 2014) or ~15–30 Mars-yr (Lapôtre and Ielpi, 2020). Such rates imply AD1 formation by potentially hundreds of fluvial floods over ~1000–10,000 Mars-yr. This conflicts with LAS counts (each at a separate height), which suggest 7–20 aggradational phases (Fig. S3). Furthermore, channel dimensions remained constant, and avulsion did not occur despite estimated avulsion frequency of ~5.7 yr (see the Supplemental Material), implying limited variation in hydrological conditions and extremely rapid aggradation. Consequently, such flow intermittency estimates are orders of magnitude too low for AD1. Median values of I on Earth are 0.1 (Hayden et al., 2021), equivalent to ~69 sol Mars-yr^{-1}; therefore, AD1 could have formed in less than 1 Mars-yr, assuming each LAP increment formed in a single flood pulse. Alternatively, an assumption of bankfull periodicity equal to 1–2 yr as on Earth (Lapôtre and Ielpi, 2020) would give ~7–40 yr. However, multiple LAPs can form during a single bankfull flow (Peakall et al., 2007), so AD1 may have formed more rapidly, in keeping with the avulsion frequency estimate.

The role of backwater hydrodynamics in creating these deposits is considered to be negligible (Nittrouer et al., 2012), since the estimated backwater length is 1.7–6.6 km (as estimated from channel depth [1.8 m] and bed slope [0.0005] measurements derived from cap-rock width [38.8 m]), and AD1 is situated ~40 km upstream (see the Supplemental Material; Fig. S7).

TRIGGER FOR BASE-LEVEL RISE

In order to examine the possible mechanisms for rapid base-level rise, we first considered the nature of the downstream basin. Resolving the remains of a downstream basin is complicated by significant resurfacing and regional tectonism (DiBiase et al., 2013; Tanaka et al., 2014). However, we used the MOLA DEM to illustrate three possible highly simplified end-member basins (a–c) based on ancient outcrops and preserved delta deposits downstream of AD1 (Fig. 1A), proximal to a large number of enclosed paleolakes (Rivera-Hernández and Palucis, 2019). We used the area of each basin to estimate the volume required to raise the water level by 6 m; i.e., the average elevation change for the deposits on AD1 (see the Supplemental Material). To raise basins a–c by 6 m would require a flood of 30–240 km^3; however, if all basins were to coexist in a chain, then 390 km^3 would be required. Given these illustrative basins, AD1 itself is unlikely to have acted as the source of water that resulted in base-level rise, as evaporative losses from the basin(s) were likely on the same order, or multiples of, the channel supplied flow, even assuming a constant bankfull flow (93.4 m^3 s^{-1}; see the Supplemental Material). Multiple channels equivalent to AD1 would have been required to fill such a basin(s), but the lack of evidence for such networks, and the aforementioned discussion around flow intermittency, indicates that this scenario is implausible (see the Supplemental Material). Instead, we suggest that a series of megafloods, sourced from

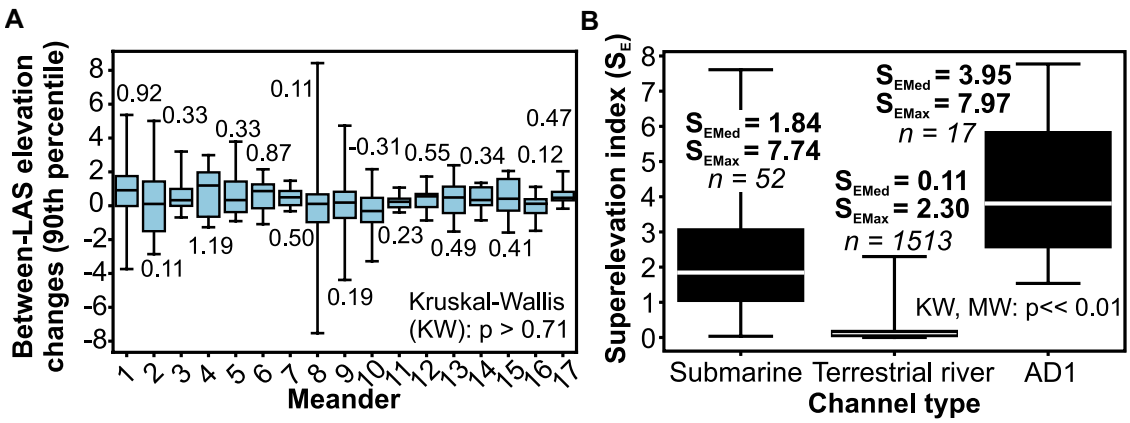

Figure 3. Lateral accretion package (LAP) characteristics on Earth and Mars. (A) Elevation changes between lateral accretion surfaces (LASs) for bends 1–17. Boxes display median and interquartile range of elevation changes between each surface of a corresponding meander. Error bars indicate the range of measurements obtained from a meander. Median measurements are displayed for each meander. Kruskal-Wallis (KW) and Mann-Whitney (MW) *U*-tests were used to compare median elevations and statistical confidence (*p*). (B) Superelevation indices (S_E) for three channel types on Earth and Mars. Boxes display median and interquartile ranges; error bars show range of S_E. Median (S_{EMed}) and maximum (S_{EMax}) values are displayed with total number of measurements (*n*).

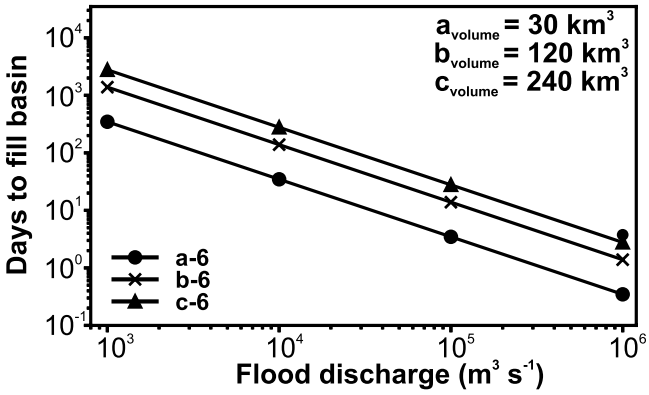

Figure 4. Estimated rates of basin filling dependent on flood volume and for different discharges. Labels a, b, and c indicate the basin being filled (see Fig. 1A), while 6 indicates the relative water elevation change (in m) required by the flood volume to match the topographic measurements on channel AD1 (Aeolis Dorsa, Mars) (Table S6 [see footnote 1]).

extrageneous reservoirs away from AD1 and capable of debouching large volumes of water over short time scales, provides a logical explanation for the creation of these deposits.

For the smallest basin (a), we estimated that the largest-magnitude megaflood (10^6 m^3 s^{-1}) could raise the basin water level by 6 m in less than a sol, while a flood of $\sim 10^3$ m^3 s^{-1} could fill the basin in <1 Mars-yr (Fig. 4). Filling times for basins b and c were estimated to range from days to a few Martian years, depending on flow rate (Fig. 4), consistent with our independent estimates of channel evolution time scales. The megafloods could have originated from crater breaches to the south of the basin (Fig. 1A), with water supplied in series as each basin was progressively filled and overspilled (e.g., Irwin et al., 2005). These volumes are modest compared to other suggested megafloods (Irwin et al., 2004). During hiatuses between megafloods, catchment-supplied sediments would have been deposited in the valleys, thus raising the level of the surrounding floodplain to the elevation of the former channel (cf. Cardenas et al., 2018) before the next flood-driven aggradational channel commenced. The channel and delta networks in Aeolis Dorsa are estimated as late Noachian or early Hesperian in age (DiBiase et al., 2013; Cardenas et al., 2018), which also aligns with independent estimates of fluvial activity across Mars (Irwin et al., 2004; Di Pietro et al., 2018). Despite widespread acceptance of fluvial activity and the formation of end-member basins across Mars during this period, we provide, for the first time, stratigraphic evidence that constrains the timing and magnitude of rapidly paced base-level rise on the planet and posit that fluvial activity and megaflooding occurred concomitantly at this time.

CONCLUSIONS

Aggradation estimates from 17 well-preserved meander lateral accretion packages on a stacked sinuous ridge in the Aeolis Dorsa were found to be more than 100% larger than any terrestrial equivalent. Stratigraphic evidence, supported by empirical relations, suggests that these deposits formed through at least two distinct phases of rapidly paced aggradation, punctuated by a topographic hiatus during which the adjacent valley was infilled by fluvially derived sediments. By combining topographic measurements with empirical relations for channel evolution, we found that the aggradational pulses may have occurred within a single Mars-year driven by a rapidly rising downstream water body. We present evidence suggesting that this base-level rise was produced by localized megaflooding sourced from breached crater lakes.

ACKNOWLEDGMENTS

We acknowledge funding received from the European Research Council (ERC) under the European Union's Horizon 2020 Research and Innovation program (GEOSTICK, Grant Agreement 725955). We thank Doug Edmonds for providing the Muscatatuck River (Indiana, USA) data and Joel Davis for producing the HiRISE digital elevation model. Na Yan and Anne Baar are thanked for discussions. We thank editor Marc Norman, Kory Konsoer, and two anonymous reviewers for their constructive reviews.

REFERENCES CITED

Blum, M.D., and Aslan, A., 2006, Signatures of climate vs. sea-level change within incised valley-fill successions: Quaternary examples from the Texas Gulf Coast: Sedimentary Geology, v. 190, p. 177–211, https://doi.org/10.1016/j.sedgeo.2006.05.024.

Buhler, P.B., Fassett, C.I., Head, J.W., III, and Lamb, M.P., 2014, Timescales of fluvial activity and intermittency in Milna Crater, Mars: Icarus, v. 241, p. 130–147, https://doi.org/10.1016/j.icarus.2014.06.028.

Cardenas, B.T., Mohrig, D., and Goudge, T.A., 2018, Fluvial stratigraphy of valley fills at Aeolis Dorsa, Mars: Evidence for base-level fluctuations controlled by a downstream water body: Geological Society of America Bulletin, v. 130, p. 484–498, https://doi.org/10.1130/B31567.1.

Constantine, J.A., Dunne, T., Ahmed, J., Legleiter, C., and Lazarus, E.D., 2014, Sediment supply as a driver of river meandering and floodplain evolution in the Amazon Basin: Nature Geoscience, v. 7, p. 899–903, https://doi.org/10.1038/ngeo2282.

Di Achille, G., and Hynek, B.M., 2010, Ancient ocean on Mars supported by global distribution of deltas and valleys: Nature Geoscience, v. 3, p. 459–463, https://doi.org/10.1038/ngeo891.

DiBiase, R.A., Limaye, A.B., Scheingross, J.S., Fischer, W.W., and Lamb, M.P., 2013, Deltaic deposits at Aeolis Dorsa: Sedimentary evidence for a standing body of water on the northern plains of Mars: Journal of Geophysical Research: Planets, v. 118, p. 1285–1302, https://doi.org/10.1002/jgre.20100.

Di Pietro, I., Ori, G.G., Pondrelli, M., and Salese, F., 2018, Geology of Aeolis Dorsa alluvial sedimentary basin, Mars: Journal of Maps, v. 14, p. 212–218, https://doi.org/10.1080/17445647.2018.1454350.

Durkin, P.R., Hubbard, S.M., Boyd, R.L., and Leckie, D.A., 2015, Stratigraphic expression of intrapoint-bar erosion and rotation: Journal of Sedimentary Research, v. 85, p. 1238–1257, https://doi.org/10.2110/jsr.2015.78.

Hayden, A.T., and Lamb, M.P., 2020, Fluvial sinuous ridges of the Morrison Formation, USA: Meandering, scarp retreat, and implications for Mars: Journal of Geophysical Research: Planets, v. 125, https://doi.org/10.1029/2020JE006470.

Hayden, A.T., Lamb, M.P., Fischer, W.W., Ewing, R.C., McElroy, B.J., and Williams, R.M.E., 2019, Formation of sinuous ridges by inversion of river-channel belts in Utah, USA, with implications for Mars: Icarus, v. 332, p. 92–110, https://doi.org/10.1016/j.icarus.2019.04.019.

Hayden, A.T., Lamb, M.P., and McElroy, B.J., 2021, Constraining the timespan of fluvial activity from the intermittency of sediment transport on Earth and Mars: Geophysical Research Letters, v. 48, https://doi.org/10.1029/2021GL092598.

Hughes, C.M., Cardenas, B.T., Goudge, T.A., and Mohrig, D., 2019, Deltaic deposits indicative of a paleo-coastline at Aeolis Dorsa, Mars: Icarus, v. 317, p. 442–453, https://doi.org/10.1016/j.icarus.2018.08.009.

Irwin, R.P., III, Howard, A.D., and Maxwell, T.A., 2004, Geomorphology of Ma'adim Vallis, Mars, and associated paleolake basins: Journal of Geophysical Research: Planets, v. 109, E12009, https://doi.org/10.1029/2004JE002287.

Irwin, R.P., III, Howard, A.D., Craddock, R.A., and Moore, J.M., 2005, An intense terminal epoch of widespread fluvial activity on early Mars: 2. Increased runoff and paleolake development: Journal of Geophysical Research: Planets, v. 110, E12S15, https://doi.org/10.1029/2005JE002460.

Jobe, Z.R., Howes, N.C., Straub, K.M., Cai, D., Deng, H., Laugier, F.J., Pettinga, L.A., and Shumaker, L.E., 2020, Comparing aggradation, superelevation, and avulsion frequency of submarine and fluvial channels: Frontiers of Earth Science, v. 8, p. 53, https://doi.org/10.3389/feart.2020.00053.

Kite, E.S., Mayer, D.P., Wilson, S.A., Davis, J.M., Lucas, A.S., and Stucky de Quay, G., 2019, Persistence of intense, climate-driven runoff late in Mars history: Science Advances, v. 5, https://doi.org/10.1126/sciadv.aav7710.

Konsoer, K.M., LeRoy, J., Burr, D., Parker, G., Jacobsen, R., and Turmel, D., 2018, Channel slope adjustment in reduced gravity environments and implications for Martian channels: Geology, v. 46, p. 183–186, https://doi.org/10.1130/G39666.1.

Lapôtre, M.G.A., and Ielpi, A., 2020, The pace of fluvial meanders on Mars and implications for the western delta deposits of Jezero Crater: American Geophysical Union Advances, v. 1, https://doi.org/10.1029/2019AV000141.

Larsen, I.J., and Lamb, M.P., 2016, Progressive incision of the Channeled Scablands by outburst floods: Nature, v. 538, p. 229–232, https://doi.org/10.1038/nature19817.

Leeder, M.R., 1973, Fluviatile fining-upwards cycles and the magnitude of palaeochannels: Geological Magazine, v. 110, p. 265–276, https://doi.org/10.1017/S0016756800036098.

Mason, J., and Mohrig, D., 2019, Scroll bars are inner bank levees along meandering river bends: Earth Surface Processes and Landforms, v. 44, p. 2649–2659, https://doi.org/10.1002/esp.4690.

McEwen, A.S., et al., 2007, Reconnaissance Orbiter's High Resolution Imaging Science Experiment (HiRISE): Journal of Geophysical Research: Planets, v. 112, E05S02, https://doi.org/10.1029/2005JE002605.

Nittrouer, J.A., Shaw, J., Lamb, M.P., and Mohrig, D., 2012, Spatial and temporal trends for water-flow velocity and bed-material sediment transport in the lower Mississippi River: Geological Society of America Bulletin, v. 124, p. 400–414, https://doi.org/10.1130/B30497.1.

Palm, F.A., Peakall, J., Hodgson, D.M., Marsset, T., Silva Jacinto, R., Dennielou, B., Babonneau, N., and Wright, T.J., 2021, Width variation around submarine channel bends: Implications for sedimentation and channel evolution: Marine Geology, v. 437, https://doi.org/10.1016/j.margeo.2021.106504.

Peakall, J., McCaffrey, B., and Kneller, B., 2000, A process model for the evolution, morphology, and architecture of sinuous submarine channels: Journal of Sedimentary Research, v. 70, p. 434–448, https://doi.org/10.1306/2DC4091C-0E47-11D7-8643000102C1865D.

Peakall, J., Ashworth, P.J., and Best, J.L., 2007, Meander-bend evolution, alluvial architecture, and the role of cohesion in sinuous river channels: A flume study: Journal of Sedimentary Research, v. 77, p. 197–212, https://doi.org/10.2110/jsr.2007.017.

Rivera-Hernández, F., and Palucis, M.C., 2019, Do deltas along the crustal dichotomy boundary of Mars in the Gale Crater region record a Northern Ocean?: Geophysical Research Letters, v. 46, p. 8689–8699, https://doi.org/10.1029/2019GL083046.

Rodriguez, J.A.P., et al., 2015, Martian outflow channels: How did their source aquifers form and why did they drain so rapidly?: Scientific Reports, v. 5, https://doi.org/10.1038/srep13404.

Tanaka, K.L., Robbins, S.J., Fortezzo, C.M., Skinner, J.A., and Hare, T.M., 2014, The digital global geologic map of Mars: Chronostratigraphic ages, topographic and crater morphologic characteristics, and updated resurfacing history: Planetary and Space Science, v. 95, p. 11–24, https://doi.org/10.1016/j.pss.2013.03.006.

USGS (U.S. Geological Survey), 2020, Mars Global Surveyor–Mars Orbiter Laser Altimeter (MOLA) Version 2 Dataset: https://astrogeology.usgs.gov/search/map/Mars/GlobalSurveyor/MOLA/Mars_MGS_MOLA_DEM_mosaic_global_463 m.

Printed in USA